ORGANIC PROCESS RESEARCH & DEVELOPMENT
OPR&D

Full Paper

An Efficient Through-Process for Chk1 Kinase Inhibitor GDC-0575

Chong Han, Keena Green, Kathrin Oehring, Arthur Meili,
Eugen Pfeifer, Michelangelo Scalone, and Francis Gosselin

Org. Process Res. Dev., **Just Accepted Manuscript** • DOI: 10.1021/acs.oprd.7b00388 • Publication Date (Web): 08 Feb 2018

Just Accepted

ACS Publications

Organic Process Research & Development is published by the American Chemical Society. 1155 Sixteenth Street N.W., Washington, DC 20036

An Efficient Through-Process for Chk1 Kinase Inhibitor GDC-0575

Chong Han,*,[†] Keena Green,[†] Kathrin Oehring,[‡] Arthur Meili,[‡] Eugen Pfeifer,[‡] Michelangelo Scalone,[‡] and Francis Gosselin[†]

[†]*Department of Small Molecule Process Chemistry, Genentech, Inc., 1 DNA Way, South San Francisco, California 94080, United States*

[‡]*Department of Pharma Technical Development, F. Hoffmann-La Roche AG, Grenzacherstrasse 124, CH-4070 Basel, Switzerland*

For Table of Content Only

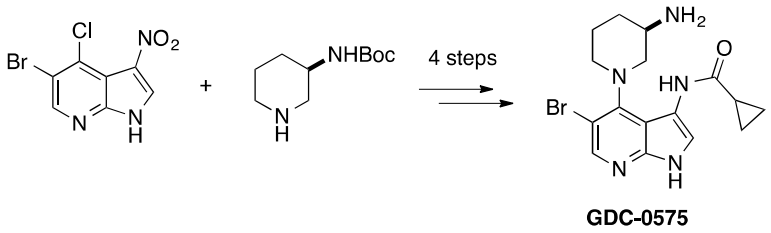

GDC-0575

Abstract

We report an efficient route to prepare Chk1 kinase inhibitor GDC-0575 from 5-bromo-4-chloro-3-nitro-7-azaindole featuring a sequence of nucleophilic aromatic substitution, hydrogenative nitro reduction, and a robust, high-yielding end-game involving deprotection-crystallization steps. The developed route was demonstrated on 10 kilogram scale in 30% overall yield to provide the target API in >99.8 A % HPLC purity.

Keywords: 7-azaindole; 3,4,5-substituted-7-azaindole; S_NAr; hydrogenative nitro reduction; Boc-deprotection.

Introduction

Checkpoint kinase 1 (Chk1) is a serine/threonine kinase that regulates cell cycle progression and is a main factor in cellular DNA damage response. Chk1 kinase inhibitors have been shown to prevent tumor cells from recovering from DNA damage induced by chemotherapeutic agents.[1] GDC-0575, a 3,4,5-substituted-7-azaindole, is a small molecule oral Chk1 inhibitor under investigation as a chemopotentiation agent for the treatment of cancer (See Scheme 1).[2] During the course of chemical development of GDC-0575 in our laboratories,[3] we required a robust synthesis on multi-kg scale with good control of the product quality of this active pharmaceutical ingredient (API) to support pharmaceutical development and clinical studies. In a previous publication, we disclosed a highly regioselective synthesis of 5-bromo-4-chloro-3-nitro-7-azaindole (**3**) harnessing the intrinsic reactivity of 7-azaindole that was demonstrated on >50 kg scale.[4] Herein, we report our development work leading to an efficient manufacturing process from azaindole **3** to GDC-0575 API.[5]

Results and Discussion

Retrosynthetic Analysis of GDC-0575. The retrosynthetic analysis is shown in Scheme 1. *N*-Boc protected GDC-0575 (**1**) would be prepared through a sequence of nitro reduction and subsequent acylation of the amine **2** from nitro-azaindole **3** that could be assembled from chloro-azaindole **4** and (*R*)-3-(Boc-amino)piperidine via a nucleophilic aromatic substitution (S_NAr) reaction.

Scheme 1. Retrosynthetic Analysis of GDC-0575

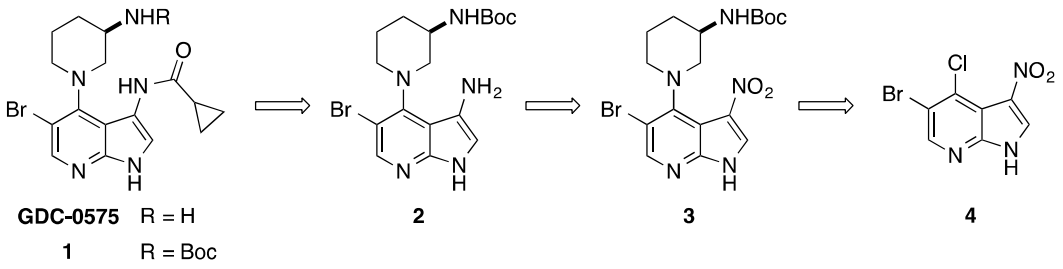

S_NAr Reaction Between Chloro-azaindole 4 and Piperidine 5. We commenced our studies on identifying a suitable transformation to prepare azaindole **3** from previously established 3-bromo-4-chloro-5-nitro-7-azaindole scaffold **4**. Due to the presence of a C-5 bromide in **4** and potential complications in terms of chemoselectivity, approaches based on transition-metal catalyzed amination were not pursued. Instead, we focused our effort on a S_NAr displacement reaction between chloro-azaindole **4** and piperidine **5** (see Table 1) taking advantage of the intrinsic activation induced by the presence of a strong electron-withdrawing nitro group at C-3.

Preliminary investigation showed that excess amounts of piperidine **5** of at least 200 mol % were required for complete conversion of the starting material **4** within a reasonable reaction time under typical S_NAr conditions in the presence of an extraneous base. Given that piperidine **5** itself can serve as a general base to neutralize the hydrogen chloride by-product, a screen of polar solvents (both protic and aprotic) was conducted using 200 mol % of **5** at 90−95 ºC in the absence of extraneous bases (Table 1, entries 1−4). We found the reaction in *t*-amyl alcohol (*t*-AmOH) gave the cleanest reaction profile with a 87% assay yield by quantitative HPLC analysis compared to reactions in other solvents such as DMSO, NMP, or 1-butanol. It is noteworthy that the reaction mixture in *t*-AmOH provided a homogeneous solution upon heating and until reaction completion. In order to maintain the homogeneity of the reaction for the benefit of reproducibility on scale, several soluble organic bases were evaluated for further optimizations.

Although no reaction rate improvement was obtained when Et_3N, *N*-methylimidazole (NMI), or pyridine was used as the base (Table 1, entries 5−7), we observed almost complete conversion (98%) using *N*-methylmorpholine (NMM) with comparable assay yield to the best condition without any extraneous bases added (Table 1, entry 8 vs entry 4). No benefits were observed when excess amounts of NMM (400 mol %) were used (Table 1, entries 9). The reaction using 100 mol % of NMM gave 98% conversion and 87% assay yield (Table 1, entries 10), which was selected as the optimal condition for further process development.[6]

Table 1. Optimization of S_NAr reaction[a]

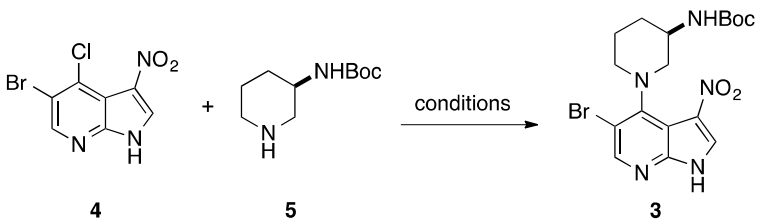

4 5 3

entry	solvent	base	conv[b] (%)	yield[c] (%)
1	DMSO	none	89	69
2	NMP	none	92	82
3	1-butanol	none	90	72
4	*t*-AmOH	none	93	87
5	*t*-AmOH	Et_3N (200 mol %)	88	78
6	*t*-AmOH	NMI (200 mol %)	85	78
7	*t*-AmOH	pyridine (200 mol %)	84	78
8	*t*-AmOH	NMM (200 mol %)	98	87
9	*t*-AmOH	NMM (400 mol %)	98	86
10	*t*-AmOH	NMM (100 mol %)	98	87

[a] Reactions conditions: Compound **4** (1.0 mmol, 100 mol %), compound **5** (200 mol %), solvent (2.8 mL), 90−95 ºC, 18 h. [b] Conversions were based on disappearance of starting material **4** by HPLC analysis. [c] Assay yield of product **3** obtained by HPLC analysis against the reference standard.

A

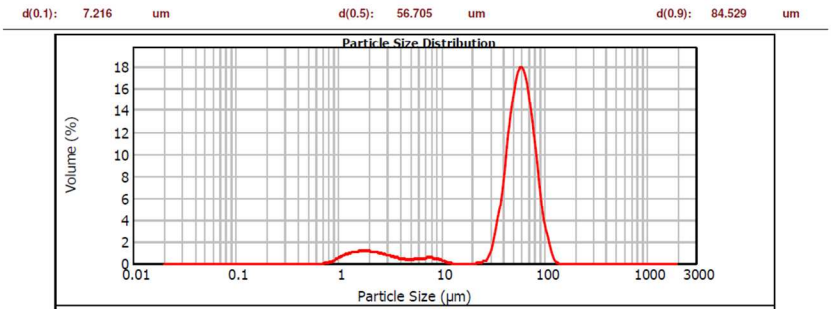

B

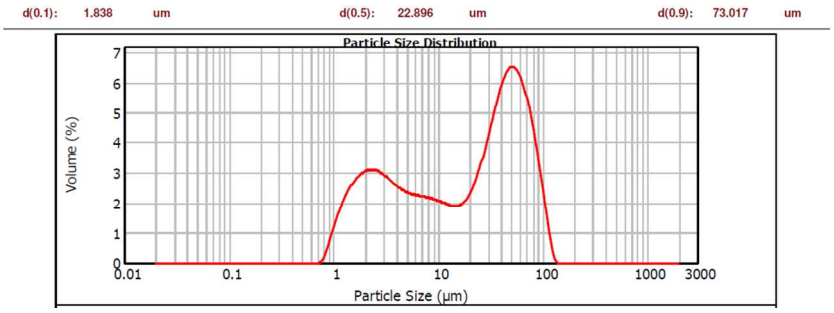

Figure 1. Particle size attrition when a slurry of compound **3** in CH_3CN was mechanically agitated. (A) PSD before aging (B) PSD after aging 15 h.

After the reaction was complete, excess amounts of nucleophile **5** could be effectively removed to <5% by aqueous citric acid washes. Owing to the low solubility of *t*-AmOH in water (99 mg/mL),[7] the layers were easily separated during the aqueous workup with no organic co-solvents required. The resulting *t*-AmOH solution was then switched to CH_3CN to isolate the desired product **3** as a crystalline solid. Although crystallization via solvent switch and the subsequent filtration proceeded uneventfully for multiple batches on up to 300 g scale, the slurry was found to exhibit paste-like consistency on multi-kg scale at the end of the crystallization. We attributed this to extended duration for the solvent switch on large scale and increased sheer

force in a baffled reactor. Particle size distribution (PSD) analysis of the solid samples revealed significant attrition of the crystals when the product slurry was deliberately agitated using an overhead mechanical stirrer over 15 h which was required to complete the solvent switch on scale (Figure 1). To overcome this issue, we designed around the original crystallization procedure involving a solvent switch and developed a cooling crystallization with seeding at 70 ºC taking advantage of the large solubility difference of the binary solvent mixture (*t*-AmOH:CH_3CN = 40:60 (v/v)) between 80 ºC and 50 ºC (132 vs 59 mg/mL; Figure 2). Because of the significant product loss in this solvent mixture even at ambient temperature, water was further introduced at 50 ºC as an additional anti-solvent to reach the final solvent composition (*t*-AmOH:CH_3CN:H_2O = 16:24:60 (v/v/v)), thus maximizing the crystallization yield. Under these crystallization conditions with particle attrition minimized, the total amount of processing time was dramatically reduced, resulting in a much improved filtration rate (ca. 30 min) on 5 kg scale.

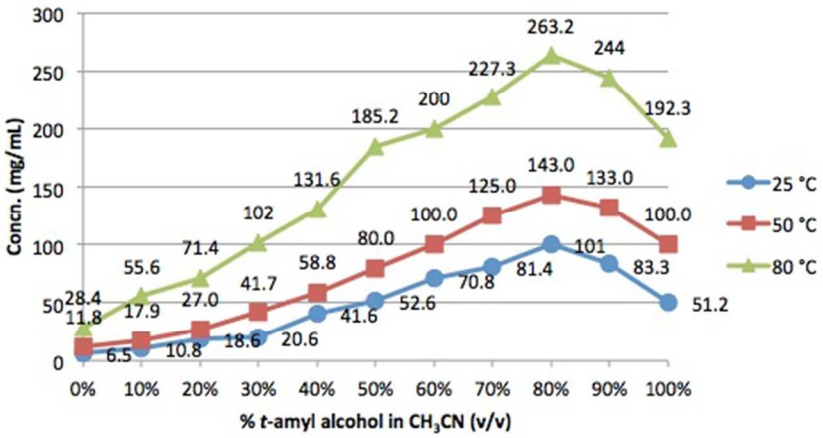

Figure 2. Solubility of compound **3** in a binary mixture of *t*-AmOH:CH_3CN

Hydrogenative Nitro Reduction and Acylation. With a reliable process in place to prepare compound **3**, we next focused our efforts on the nitro reduction step aiming at developing a chemoselective transformation to afford amino-azaindole **2** without competing hydrogenolysis of

the 5-bromo substituent (Table 2). The desired amino-azaindole product **2** was found to be extremely oxygen-sensitive, rapidly decomposing to azaisatin **6**[8] (Figure 3; confirmed by LCMS analysis) and other unidentified side products upon exposure to air, which made analysis of the reaction profile quite challenging. To overcome this stability issue and reliably analyze the reaction profile, the resulting reaction mixture after completion of the nitro reduction was immediately quenched with a cyclopropanecarbonyl acylating reagent in the same pot after exchanging out the hydrogen with an inert gas such as nitrogen or argon. Filtering off the heterogeneous catalyst in a glovebox before the addition of an acylating reagent did not show any advantage in terms of the impurity profile or the assay yield of product **1** by quantitative HPLC analysis.

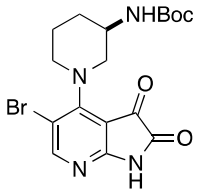

6

Figure 3. Azaisatin-type impurity **6** derived from oxidative decomposition of amino-azaindole **2**

With respect to the catalyst selection, Pt- over Pd-based heterogeneous catalysts were deliberately chosen for evaluation to minimize the competitive hydrogenolysis of the 5-Br group, while promoting the desired nitro reduction.[9] Several commercially available heterogeneous platinum catalysts with metal modifiers such as 1% Pt−2% V/C, 3% Pt−0.3% Cu/C, and 5% Pt−0.5% Fe/C were examined, and 1% Pt−2% V/C was found to be optimal based on the reaction performance and the catalyst loading. A preliminary screen of reaction pressure and temperature showed no benefit of a higher pressure than 5 atm but a faster rate at 50 ºC compared to 25 ºC. Therefore, the reaction conditions using 15 wt % of 1% Pt−2% V/C as the

catalyst, under 5 atm of hydrogen, at 50 ºC in 2-methyltetrahydrofuran (MeTHF) were selected for further optimizations.

Table 2. Optimization of Nitro Reduction and Acylation Steps

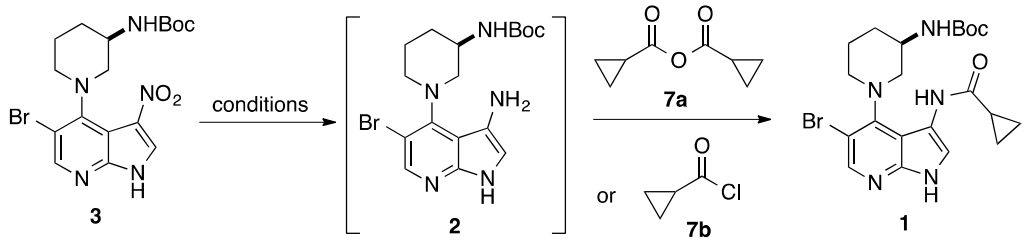

entry[a]	base	additive (mol %)	acylating reagent	solvent	1[b] (%)	yield[c] (%)
1	None	None	**7a**	MeTHF	70	57
2	K_2CO_3	None	**7a**	MeTHF	70	58
3	Et_3N	None	**7a**	MeTHF	87	65
4	DABCO	None	**7a**	MeTHF	92	74
5	TMEDA	None	**7a**	MeTHF	90	74
6	NMM	None	**7a**	MeTHF	90	74
7	NMM	None	**7b**	MeTHF	88	71 (67)
8	NMM	None	**7b**	*t*-AmOH	76	67
9	NMM	None	**7b**	*t*-AmOH:H_2O = 95:5	87	79
10	NMM	None	**7b**	*t*-AmOH:H_2O = 90:10	87	81 (75)
11	NMM	None	**7b**	*t*-AmOH:H_2O = 80:20	90	81
12	NMM	**5** (100)	**7b**	*t*-AmOH:H_2O = 90:10	93	82
13	NMM	citric acid (5 wt %)	**7b**	*t*-AmOH:H_2O = 90:10	86	76
14	NMM	B(O*i*-Pr)$_3$ (100)	**7b**	*t*-AmOH:H_2O = 90:10	85	71
15	NMM	HCl (66)	**7b**	*t*-AmOH:H_2O = 90:10	88	79

[a] Reactions conditions: compound 3 (5 mmol), 1% Pt−2% V/C (16 wt %), H_2 (5 atm), base (170 mol %), solvent (1.0 M), 50 ºC, 2−5 h; then acylating reagent **7a** or **7b** (150 mol %), 0 ºC. [b] Area percentage of compound 1 based on HPLC analysis. [c] Assay yield against a reference standard determined by HPLC analysis. Isolated yields with potency corrected for both starting material and product are shown in parentheses.

At first, employing the symmetrical anhydride **7a** as the acylating reagent, the desired product **1** was obtained in 57% assay yield (70 A % HPLC) through the sequence of hydrogenative nitro reduction and subsequent acylation in MeTHF (Table 2, entry 1). Examination of the addition of the base before or after the nitro reduction revealed a beneficial effect when the base was present during the nitro reduction step. A number of bases including K_2CO_3, Et_3N, DABCO, TMEDA, and NMM were next evaluated for the hydrogenative nitro reduction and acylation sequence using **7a** (Table 2, entries 2−6). DABCO, TMEDA, and NMM showed superior reaction conversion and assay yield of product **1** by quantitative HPLC analysis over other bases (Table 2, entries 4−6). Switching the acylating reagent from the symmetrical anhydride **7a** to the corresponding acid chloride **7b** resulted in a slight decrease in the assay yield of **1** (71% vs 74%; Table 2, entry 7 vs 6**)**, which was compensated by the commercial availability and lower cost of **7b**. With the objective of developing a telescoped process in mind, the hydrogenation reaction was also evaluated in solvents used for the S_NAr step. Although the reactions in pure *t*-AmOH afforded a lower assay yield compared to the ones performed in MeTHF using acid chloride **7b** (Table 2, entry 8 vs entry 7), addition of 5−20% (v/v) water to the *t*-AmOH significantly boosted the assay yield by ca. 10% (ca. 80% vs 71%; Table 2, entries 9−11 vs entry 7) and the acylation step was found to be compatible with 5−20% (v/v) of water present as a co-solvent. Examination of the impact of potential carried-over impurities from the S_NAr step, namely residual piperidine **5** starting material and citric acid from the aqueous workup, on the performance of the nitro reduction showed no negative effect when 100 mol % of piperidine **5** or 5 wt % of citric acid was

spiked (Table 2, entries 12 and 13). Attempts to improve the yield of **1** by stabilizing the oxygen-sensitive amino-azaindole **2** using Brønsted or Lewis acids did not show any promise (Table 2, entries 14 and 15). Under the optimized conditions, product **1** was isolated in a 67% or 75% yield, respectively, using MeTHF or a 90:10 (v/v) mixture of *t*-AmOH and water as the solvent.

Development of a 3-Step Through-Process. Further process development identified a crystallization procedure after filtering off the heterogeneous catalyst and aqueous workup to afford compound **1** as a highly crystalline 1:1 toluene solvate[10] (Figure 4), which exhibited exceptional purging power on process-related organic impurities, upgrading the product purity from 87 A % HPLC in the crude reaction mixture after workup to >99.5 A % HPLC in the isolated **1**•toluene. The robustness of this crystallization, in conjunction with the earlier reaction optimization work on the hydrogenation step, led us to examine the possibility of developing a 3-step telescoped sequence from the S_NAr step to compound **1**, obviating the need for a cumbersome isolation of the nitro-azaindole intermediate **2** and further streamlining the process.

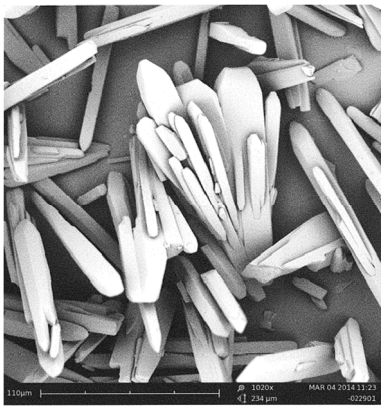

Figure 4. SEM image of **1•toluene** (1020× magnification)

To examine the feasibility of the proposed telescoped process, we began with evaluating whether the purity of the isolated compound **1** through the telescoped process would compare to the one via the established stepwise process (Scheme 2). The S_NAr reaction mixture after

aqueous washes typically contained ca. 10% water, matching the solvent composition under the optimized conditions for the hydrogenation step (See Table 2, entry 10). This compound **2**-containing mixture in *t*-AmOH/H_2O was then subjected to the previously established hydrogenation conditions using 15 wt % of 1% Pt−2% V/C as the catalyst, NMM as the base additive, under 5 atm of hydrogen, at 50 ºC. After the complete consumption of the nitro-azaindole starting material **2**, the reaction mixture was cooled to 0 ºC and treated with cyclopropanecarbonyl chloride to provide the product **1**. The resulting mixture was then filtered to remove the heterogeneous catalyst and subjected to aqueous workup. The resulting organic solution was then solvent-switched to toluene to isolate the product **1** as a toluene solvate. Gratifyingly, the purity of product **1** from the telescoped process was found to be >99.5 A % HPLC over multiple batches on the scale ranging from g to kg, which was comparable to the high product purity from the original stepwise process.

Scheme 2. A 3-Step Telescoped Process to Produce Compound 1

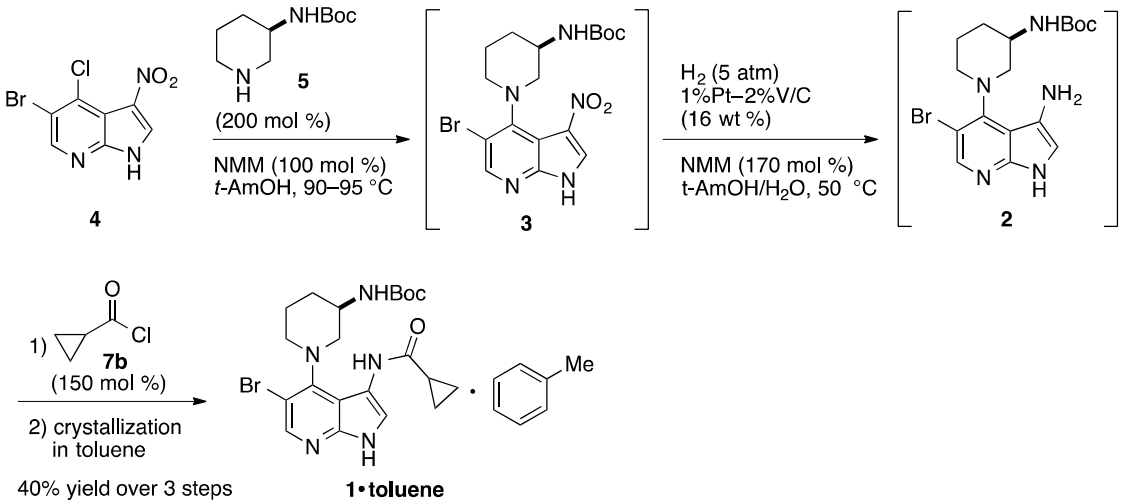

Boc Deprotection and Final API Crystallization. With a reliable telescoped process to produce the penultimate intermediate **1** in a >99.5 A % HPLC purity, we moved on to the final

Boc deprotection step. Two common mineral acids, hydrochloric acid and sulfuric acid, gave complete conversions removing the Boc group in THF or alcohol solvents. Considering the potential formation of chloroalkanes genotoxic impurities (GTI) when hydrochloric acid was used in combination with alcohol solvents or THF,[11] sulfuric acid was chosen for further development. After examining the stoichiometry and concentration of sulfuric acid, we settled on using 300 mol % of 4.5 M H_2SO_4 in order to achieve a >99.5% conversion that was needed to control the level of **1** in the isolated API because of inefficient purging in downstream processing.

Scheme 3. Proposed Pathways for the Formation of Oxidative Impurities from GDC-0575

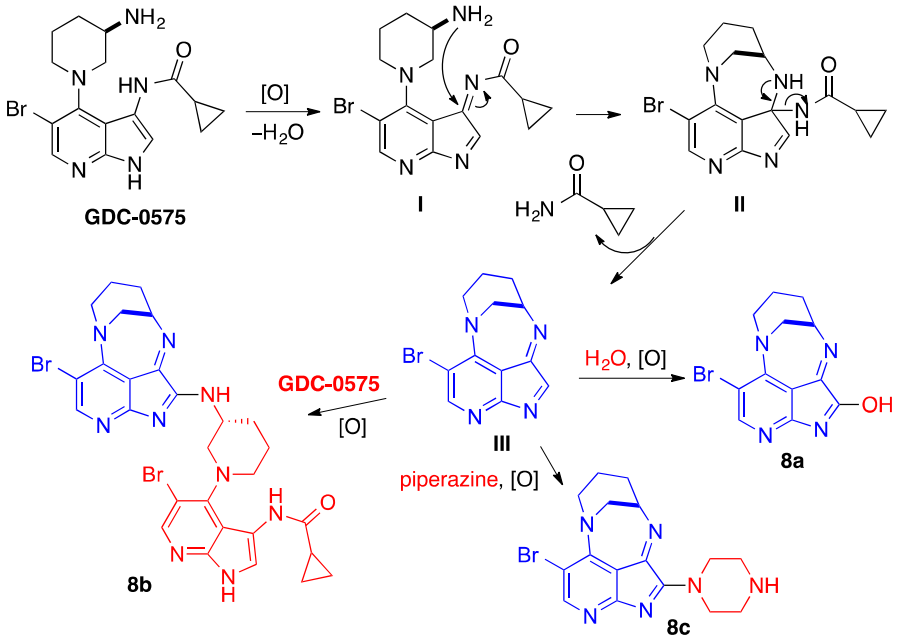

Since the free base of the GDC-0575 was selected as the final API form, we desired a process involving free-basing the sulfate salts after Boc deprotection under acidic conditions and obtaining the freebase as an organic solution where a polish filtration could be performed to remove insoluble particulates, followed by final crystallization to obtain the API in high purity. Following this design, solubility screen of the API freebase in a host of organic solvents

identified THF as the only hit providing decent solubility (>50 mg/mL) while a phase cut would be feasible upon an aqueous workup to remove the water-soluble salts and by-products. However, we observed the formation of several API related impurities at <1 A % level during the free-basing step under basic conditions, with one of which (**8b**) showing poor purging in downstream processing. Therefore, the formation of **8b** needed to be prevented. The structures of the observed impurities were proposed based on HRMS and NMR spectroscopic analysis with the postulated pathways for their formation depicted in Scheme 3. Upon oxidative cyclization of the free primary amine onto C-3 and subsequent expulsion of cyclopropylcarboxamide, the intermediate **III** is prone to nucleophilic attack at C-2 leading to impurity **8a** with hydroxide being the nucleophile and impurity **8b** with another molecule of API being the nucleophile.

To better understand the API impurity formation, we performed stability studies under basic conditions. The level of impurity **8b** showed a clear dependence on the pH of the basic solution at 25 ºC, with 2.72 A % increase using 0.1 N NaOH, 0.51 A % increase using 0.01 N NaOH, and 0.16 A % increase observed even using a 20 wt % K_2HPO_4 solution (pH = ca. 8.5) that could barely free-base the API. The postulated impurity formation pathways suggested use of a sacrificial amine nucleophile that could compete with the primary amine in the API to attack intermediate III, resulting in a more polar adduct that could be purged as effectively as the hydroxyl adduct **8a**. We thus selected piperazine as a highly water-soluble amine for evaluation. Gratifyingly, the formation of **8b** was effectively inhibited to <0.05 A % at 60 ºC in a mixture of THF/H_2O or EtOH/H_2O that were the solvents used for the downstream process including the API crystallization. As expected, the corresponding piperazine adduct **8c** could be easily purged in the EtOH/H_2O system during crystallization.

Scheme 4. Boc Deprotection and API Crystallization to GDC-0575

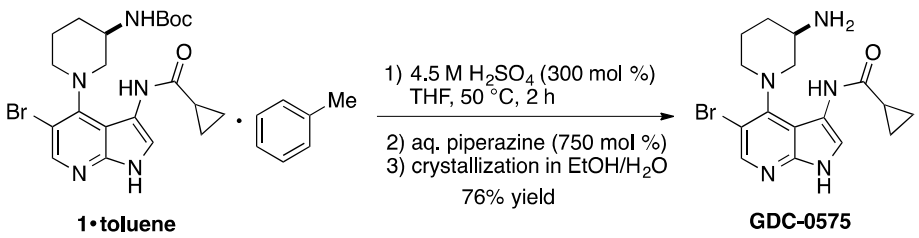

With the aqueous piperazine solution identified to free-base the API cleanly, the resulting process stream in THF was polish filtered and solvent-switched to a mixture of EtOH/H_2O to crystallize the GDC-0575 as a freebase in >99.8 A% HPLC purity (Scheme 4). Three observed impurities including aforementioned **8a** and **8b**, and impurity **8d** derived from hydrolysis of **8b**, were each well controlled at <0.10A% HPLC in isolated GDC-0575 API (Figure 5).

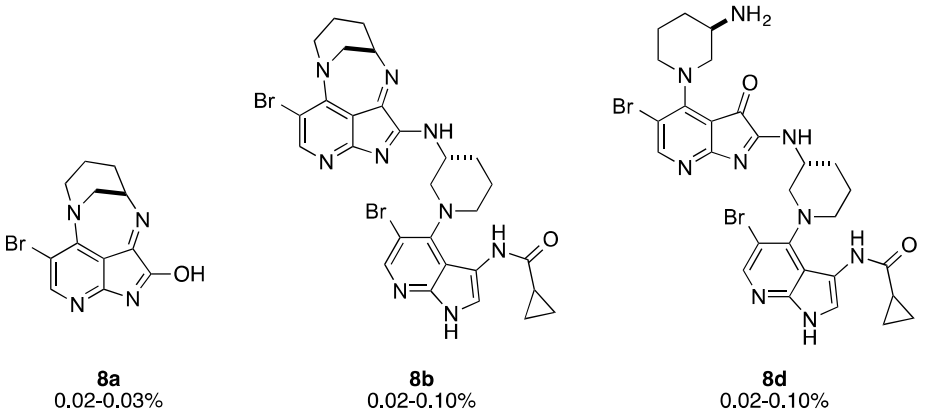

Figure 5. Observed impurities in isolated GDC-0575

Conclusion

In summary, we developed a highly efficient process to prepare GDC-0575 starting from the previously reported 5-bromo-4-chloro-3-nitro-7-azaindole (**3**). The synthesis featured a 3-step through-process sequence including a chemoselective hydrogenative nitro-reduction using a Pt–V/C catalyst, and a high-yielding Boc deprotection–API crystallization step involving use of an aqueous piperazine solution to obtain the API freebase with excellent control of the impurity profile. The

developed process was demonstrated on multi-kg scale successfully producing the final API in 30% yield and >99.8 A % HPLC purity.

Experimental Section

General Information. All reactions were performed under a nitrogen atmosphere unless otherwise stated. Unless otherwise noted, NMR spectra were recorded on a Bruker 300 MHz instrument at ambient temperature. All ^{1}H NMR spectra were measured in parts per million (ppm) relative to the residual solvent peak in the deuterated solvent (δ 2.50 for DMSO-d_6). Data for ^{1}H NMR spectra are reported as follows: chemical shift (δ ppm), multiplicity (br = broad, s = singlet, d = doublet, t = triplet, q = quartet, m = multiplet), coupling constant (Hz), and integration. All ^{13}C NMR spectra are reported in ppm relative to the deuterated solvent peak (δ 39.5 ppm for DMSO-d_6) and were obtained with complete ^{1}H decoupling unless otherwise stated. HRMS data was obtained on a LTQ Orbitrap Discovery (Thermo Fisher Scientific) at Genentech, Inc. Melting points were measured by differential scanning calorimetry (DSC, TA Instruments Q2000) and reported as onset temperature. The heterogeneous Pt-based catalysts were purchased from Evonik, AG.

*(R)-5-Bromo-4-(3-(tert-butoxycarbonylamino)piperidin-1-yl)-3-nitro-1H-pyrrolo[2,3-b]pyridine (**3**)*. A mixture of 5-bromo-4-chloro-3-nitro-1*H*-pyrrolo[2,3-*b*]pyridine **4** (24.4 kg, 88.3 mol, 100 mol %), (*R*)-*tert*-butyl piperidin-3-ylcarbamate **5** (35.4 kg, 177 mol, 200 mol %), *N*-methylmorpholine (9.05 kg, 89.5 mol, 101 mol %), and 2-methyl-2-butanol (270 kg) was stirred at 85±5 °C for 21 h and cooled to 25 °C. The mixture was then washed with 10 wt % citric acid aqueous solution (244 kg) and water (244 kg). The resulting organic phase was diluted with 2-methyl-2-butanol (73.2 kg) to give a solution of (*R*)-5-bromo-4-(3-(tert-

butoxycarbonylamino)piperidin-1-yl)-3-nitro-1*H*-pyrrolo[2,3-b]pyridine (**3**) (276 kg, 11.1 wt % in in 2-methyl-2-butanol, H_2O content by KF: 12.2%, 79% yield), which was used directly in the next step. An analytical sample of (*R*)-5-bromo-4-(3-(*tert*-butoxycarbonylamino)piperidin-1-yl)-3-nitro-1*H*-pyrrolo[2,3-*b*]pyridine **(3)** was obtained by crystallization from CH_3CN: yellow solid; mp = 208 °C; ^{1}H NMR (600 MHz, DMSO-d_6) δ 13.12 (s, 1H), 8.60 (s, 1H), 8.39 (s, 1H), 6.80 (d, J = 6.8 Hz, 1H), 3.49 (m, 1H), 3.34 (m, 2H), 3.22 (t, J = 11.2 Hz, 1H), 3.00 (t, J = 10.2 Hz, 1H), 1.88 (dd, J = 12.3, 2.8 Hz, 1H), 1.74 (m, 2H), 1.38 (m, 1H), 1.34 (s, 9H); ^{13}C NMR (150 MHz, DMSO-d_6) δ 154.8, 148.9, 148.2, 147.9, 130.6, 128.5, 113.8, 109.6, 77.6, 54.7, 48.9, 47.3, 30.0, 28.1 (3C), 24.2; HRMS–ESI (*m*/*z*): $[M + H]^+$ calcd for $C_{17}H_{23}BrN_5O_4$, 440.0928; found, 440.0912.

*(R)-5-Bromo-4-(3-(tert-butoxycarbonylamino)piperidin-1-yl)-3-(cyclopropanecarboxamido)-1H-pyrrolo[2,3-b]pyridine (**1**•toluene).* To an inerted stainless steel pressure reactor were charged (*R*)-5-bromo-4-(3-(*tert*-butoxycarbonylamino)piperidin-1-yl)-3-nitro-1*H*-pyrrolo[2,3-*b*]pyridine (275.7 kg @ 11.1 wt% in 2-methyl-2-butanol, 30.6 kg, 69.5 mol, 100 mol %), 1% Pt + 2% V/C (4.58 kg, wet weight, 15 wt %), *N*-methylmorpholine (11.9 kg, 118 mol, 170 mol %), and 2-MeTHF (140.4 kg). The reaction mixture was degassed through vacuum-purge cycles with N_2 and then pressurized to 5 bar H_2 and stirred at 50 ºC for a minimum of 2 h. The autoclave was emptied and the mixture was transferred with a MeTHF rinse (2 × 20.8 kg). The batch was cooled to 0–10 ºC and cyclopropanecarbonyl chloride (11.0 kg, 105 mol, 152 mol %) was charged into the reactor over 1 h. The reaction mixture was stirred at 25 ºC for 4 h and filtered through Celite. The cake was washed with 2-MeTHF (4 × 24.7 kg). The filtrate was washed with NH_4Cl solution (28.1 kg) in H_2O (156 kg). The organic layer was washed with H_2O (183.1 kg) and then distilled at 40–60 ºC under vacuum to 1/3 of its original volume. Toluene (680.9 kg)

was added and the batch was distilled until 2-methyl-2-butanol was ≤3.0 wt %. The batch was cooled to 15–25 ºC and the resulting solid was isolated by centrifugation, washed with 3 portions of toluene (total: 142.2 kg) and dried in a at 40 ºC overnight to give (*R*)-5-bromo-4-(3-(*tert*-butoxycarbonylamino)piperidin-1-yl)-3-(cyclopropanecarboxamido)-1*H*-pyrrolo[2,3-*b*]pyridine **(1)**•toluene (21.1 kg, 50% yield) as an off-white solid: mp = 135 °C; ^{1}H NMR (600 MHz, THF-d_8, 4 ºC) δ 10.76 (s, 1H), 9.72 (s, 1H), 8.15 (s, 1H), 7.90 (d, *J* = 2.4 Hz, 1H), 7.18–7.08 (m, 5H), 6.41 (d, *J* = 7.8 Hz, 1H), 3.82 (m, 1H), 3.60 (m, 1H), 3.44 (t, *J* = 10.6 Hz, 1H), 3.30 (dd, *J* = 10.6, 3.9 Hz, 1H), 3.03 (d, *J* = 10.9 Hz, 1H), 2.29 (s, 3H), 2.08 (m, 1H), 1.89 (m, 2H), 1.66 (m, 1H), 1.37 (s, 9H), 1.36 (m, 1H), 0.95–0.80 (m, 4H); ^{13}C NMR (150 MHz, THF-d_8, 4 ºC) δ 170.1, 155.8, 149.0, 147.8, 147.6, 138.4, 129.6 (2C), 128.9 (2C), 126.0, 116.6, 115.6, 111.9, 108.8, 78.5, 55.8, 50.2, 49.1, 31.8, 28.6 (3C), 26.3, 21.5, 15.8, 7.7, 7.6; HRMS–ESI (*m*/*z*): $[M + H]^+$ calcd for $C_{21}H_{29}BrN_5O_3$, 478.1448; found, 478.1431.

(R)-5-Bromo-4-(3-amino)piperidin-1-yl)-3-(cyclopropanecarboxamido)-1H-pyrrolo[2,3-b]pyridine (GDC-0575). To an inerted reactor equipped with a mechanical stirrer, a nitrogen / vacuum manifold, a thermocouple, and a condenser, were charged (*R*)-5-bromo-4-(3-(*tert*-butoxycarbonylamino)piperidin-1-yl)-3-nitro-1*H*-pyrrolo[2,3-*b*]pyridine•toluene (10.3 kg, 17.6 mol, 100 mol %), THF (273.7 kg), followed by H_2SO_4 (14.4 kg, 36 wt %, 52.9 mol, 300 mol %). The reaction mixture was stirred at 50 °C for 2 h and then cooled to 20 °C. A degassed aqueous solution of piperazine (11.7 kg, 136 mol, 770 mol %) in H_2O (65.4 kg) was added slowly while maintaining the internal temperature at 15–30 °C. The batch was stirred for 30 min and the bottom aqueous layer was discarded. To the organic layer was added degassed EtOH (131.8 kg) and the batch was line-filtered and distilled under vacuum at 50 ºC until THF ≤10 wt %. Line-filtered, degassed H_2O (68.3 kg) was added at 50 °C over 1 h and the batch was cooled to 20 ºC

over 3 h. The resulting solid was isolated by filtration, washed with degassed solution of EtOH (12.6 kg) in water (29.8 kg) and dried in a vacuum oven at 50 ºC overnight to give (*R*)-5-bromo-4-(3-amino)piperidin-1-yl)-3-(cyclopropanecarboxamido)-1*H*-pyrrolo[2,3-*b*]pyridine as a light yellow solid (5.1 kg, 76% yield, 99.9 A % by HPLC analysis). Both ^{1}H and ^{13}C spectra of GDC-0575 freebase are very broad. Therefore, the spectra shown below are of freebase converted to a bis-HCl salt: mp = 267 °C; ^{1}H NMR (300 MHz, DMSO-d_6): δ 11.98 (br, 1H), 9.78 (s, 1H), 8.44 (br, 3H), 8.25 (s, 1H), 7.45 (d, J = 2.4 Hz, 1H), 3.57 (m, 1H), 3.43 (m, 1H), 3.41 (m, 1H), 3.28 (m, 1H), 3.14 (m, 1H), 2.15 (m, 1H), 1.90 (penta, J = 6.5 Hz, 1H), 1.81 (m, 1H), 1.72 (m, 1H), 1.52 (m, 1H), 0.83 (m, 4H); ^{13}C NMR (75 MHz, DMSO-d_6): δ 172.9, 149.5, 145.9, 145.1, 121.9, 114.2, 113.1, 107.8, 53.8, 51.1, 47.5, 28.6, 24.37, 14.7, 7.55, 7.45; HRMS–ESI (m/z): $[M + H]^+$ calcd for $C_{16}H_{21}BrN_5O$, 378.0924; found, 378.0912.

Associated Contents

Supporting Information. The supporting information is available free of charge on the ACS Publications website.

^{1}H and ^{13}C NMR spectra of compounds **3**, **1**, and **GDC-0575.**

Author Information

Corresponding Author

*E-mail: han.chong@gene.com

Notes

The authors declare no competing financial interest.

Acknowledgements

We thank Dr. Haiming Zhang for helpful discussion, Dr. Chunang Gu for collecting HRMS data, Dr. David Russell for obtaining NMR data, Dr. Jane Li, Mr. Hong Lin, Ms. Stephanie Gee for analytical support, and Ms. Rebecca Rowe for collecting mp data (Genentech, Inc.). We also thank all colleagues in the analytical department in Basel for their valuable analytical support.

References

[1] Lainchbury, M.; Collins, I. *Expert Opin. Ther. Patents* **2011**, *21*, 1191−1210.

[2] Blake, J. F.; Guanawardana, I. W.; Huerou, Y. L.; Mohr, P. J.; Wallace, E. M; Wang, B.; Chicarelli, M. J.; Leon, M. Pyrrolopyridines as Kinase Inhibitors. U.S. Patent 8,178,131, May 15, 2012.

[3] Blake, J. F.; Guanawardana, I. W.; Huerou, Y. L.; Mohr, P. J.; Wallace, E. M; Wang, Bin U.S. Patent, 8,841,304, 2014.

[4] Han, C.; Green, K.; Pfeifer, E.; Gosselin, F. *Org. Process Res. Dev.* **2017**, *21*, 664−668.

[5] Han, C.; Green, K.; Gosselin, F., Scalone, M.; Nichols, P. J.; Liu, W.; Spencer, K. L.; Crane, Z. D.; Stengel, P. J. U.S. Patent Application, 20160200723, 2016.

[6] Differential Scanning Calorimetry (DSC) analysis of the crude reaction mixture from 20 ºC to 350 ºC at a rate of 10 ºC/min using a high pressure gold plated crucible showed a mild exotherm of 145 J/g with an onset temperature at 228 ºC, indicating the reaction is safe to be performed at 95 ºC with a safety margin of 130 ºC. Similar analysis of the isolated compound **3** showed a exotherm of 532 J/g with an onset temperature at 218 ºC. A safety margin of approximately 150 ºC was built in under the drying conditions at 70 ºC.

[7] Yalkowsky, S. H.; He, Y.; Jain P. *Handbook of Aqueous Solubility Data,* 2nd Ed.; CRC Press: Boca Raton, FL, 2010; p 184.

[8] For oxidation of indole to isatin, see: Zi, Y.; Cai, Z.-J.; Wang, S.-Y.; Ji, S.-J. *Org. Lett.* **2014**, *16*, 3094−3097 and references therein.

[9] For a recent review, see: Orlandi, M.; Brenna, D.; Harms, R.; Jost, S.; Benaglia, M. *Org. Process Res. Dev.* **2017**, Just Accepted Manuscript. DOI: 10.1021/acs.oprd.6b00205.

[10] The toluene content of compound **1** was found to be within the range of 15.4–16.0% (w/w) for multiple development and manufacturing batches as opposed to a theoretical 16.2% (w/w) for the 1:1 toluene solvate.

[11] Snodin, D. J. *Org. Process Res. Dev.* **2010**, *14*, 960−976.